



ELSEVIER

Available online at [www.sciencedirect.com](http://www.sciencedirect.com)

SCIENCE @ DIRECT®

PHYSICS LETTERS B

Physics Letters B 590 (2004) 133–142

[www.elsevier.com/locate/physletb](http://www.elsevier.com/locate/physletb)

# Dynamics of antiproton cooling in a positron plasma during antihydrogen formation

ATHENA Collaboration

M. Amoretti<sup>a</sup>, C. Amsler<sup>b</sup>, G. Bonomi<sup>c</sup>, A. Bouchta<sup>c</sup>, P.D. Bowe<sup>d</sup>, C. Carraro<sup>a,e</sup>,  
C.L. Cesar<sup>f</sup>, M. Charlton<sup>d</sup>, M. Doser<sup>c</sup>, V. Filippini<sup>g,h</sup>, A. Fontana<sup>g,h</sup>, M.C. Fujiwara<sup>i</sup>,  
R. Funakoshi<sup>j</sup>, P. Genova<sup>g,h</sup>, J.S. Hangst<sup>k</sup>, R.S. Hayano<sup>j</sup>, L.V. Jørgensen<sup>d</sup>,  
A. Kellerbauer<sup>c</sup>, V. Lagomarsino<sup>a,e</sup>, R. Landua<sup>c</sup>, D. Lindelof<sup>b</sup>, E. Lodi Rizzini<sup>l</sup>,  
M. Macrí<sup>a</sup>, N. Madsen<sup>k</sup>, G. Manuzio<sup>a,e</sup>, P. Montagna<sup>g,h</sup>, H. Pruys<sup>b</sup>, C. Regenfus<sup>b</sup>,  
A. Rotondi<sup>g,h</sup>, G. Testera<sup>a</sup>, A. Variola<sup>a,\*</sup>, L. Venturelli<sup>l</sup>, D.P. van der Werf<sup>d</sup>,  
Y. Yamazaki<sup>i</sup>

<sup>a</sup> *Istituto Nazionale di Fisica Nucleare, Sezione di Genova, 16146 Genova, Italy*

<sup>b</sup> *Physik-Institut, University of Zurich, 8057 Zürich, Switzerland*

<sup>c</sup> *Department of Physics, CERN, 1211 Geneva 23, Switzerland*

<sup>d</sup> *Department of Physics, University of Wales Swansea, Swansea SA2 8PP, UK*

<sup>e</sup> *Dipartimento di Fisica, Università di Genova, 16146 Genova, Italy*

<sup>f</sup> *Instituto de Física, Universidade Federal do Rio de Janeiro, Rio de Janeiro 21945-970, Brazil*

<sup>g</sup> *Istituto Nazionale di Fisica Nucleare, Sezione di Pavia, 27100 Pavia, Italy*

<sup>h</sup> *Dipartimento di Fisica Nucleare e Teorica, Università di Pavia, 27100 Pavia, Italy*

<sup>i</sup> *Atomic Physics Laboratory, RIKEN, Saitama 351-0198, Japan*

<sup>j</sup> *Department of Physics, University of Tokyo, Tokyo 113-0033, Japan*

<sup>k</sup> *Department of Physics and Astronomy, University of Aarhus, 8000 Aarhus C, Denmark*

<sup>l</sup> *Dipartimento di Chimica e Fisica per l'Ingegneria e per i Materiali, Università di Brescia, 25123 Brescia, Italy*

Received 27 February 2004; accepted 23 March 2004

Available online 6 May 2004

Editor: W.-D. Schlatter

## Abstract

We demonstrate cooling of  $10^4$  antiprotons in a dense, cold plasma of  $\sim 10^8$  positrons, confined in a nested cylindrical Penning trap at about 15 K. The time evolution of the cooling process has been studied in detail, and several distinct types of behavior identified. We propose explanations for these observations and discuss the consequences for antihydrogen production. We contrast these results with observations of interactions between antiprotons and “hot” positrons at about 3000 K, where antihydrogen production is strongly suppressed.

© 2004 Elsevier B.V. All rights reserved.

PACS: 52.40.Mj; 36.10.-k; 52.20.Hv; 52.27.Jt

0370-2693/\$ – see front matter © 2004 Elsevier B.V. All rights reserved.

doi:10.1016/j.physletb.2004.03.073

*Keywords:* Antihydrogen; Cooling; Nested trap; Positron plasma; Antiprotons

## 1. Introduction

In 2002 ATHENA Collaboration announced the first production and detection of antihydrogen atoms at cryogenic temperature [1]. Another experiment subsequently reported observing antihydrogen [2]. These results open the door to fundamental investigations of the properties of neutral, antiatomic matter. Spectroscopic comparisons of hydrogen and antihydrogen can provide sensitive tests of CPT symmetry, and the first investigation of the behavior of antimatter in a gravitational field can be contemplated.

In ATHENA antihydrogen is produced by mixing a cloud of antiprotons with a positron plasma in an electromagnetic trap. The expected reaction mechanisms favor low relative velocities, the rates for the radiative and three-body processes varying as  $T^{-0.63}$  and  $T^{-4.5}$ , respectively [3]. Since at thermal equilibrium the velocity scales as the square root of the mass, a good approximation is to consider  $T$  as the positron plasma temperature. To obtain low relative antiproton and positron velocities, we exploit the low mass of the latter. In a high magnetic field, positrons rapidly lose energy by synchrotron radiation and come into thermal equilibrium with the surroundings. The cooling time constant in the 3 T field in ATHENA is about 0.5 s; the ambient temperature is about 15 K. Antiprotons can then be sympathetically cooled by the positrons, if the two clouds of particles are permitted to interact.

Here we demonstrate cooling of “slow” ( $\sim 30$  eV) antiprotons by a dense, spheroidal cloud of positrons. The cooling is monitored for various interaction times by destructive measurements of the energy distribution of the remaining antiprotons. The result is a complete record of the cooling process that provides a more comprehensive description than has hitherto been available [2,4,5]. Furthermore, we are able to correlate the evolution of the cooling process with that of the trigger rate of our unique antihydrogen annihilation detector [6]. This establishes, for the first time, a link between antiproton cooling dynamics in a nested

potential configuration and the production of cold antihydrogen.

It is also important to note that, although the antiproton numbers are similar, the ratio of positrons to antiprotons is about  $10^4$  in the current experiment, compared to about 60 in the earlier work [4]. Thus, forces due to the space charge of the positron clouds are important to the dynamics of the cooling, and the time scales involved are very different from those observed previously [2,4].

## 2. Antihydrogen production

The ATHENA antihydrogen apparatus [7] consists of four parts: a positron accumulator, an antiproton catching trap, a mixing trap and an antihydrogen detector. In the positron accumulator [9] about  $1.5 \times 10^8$  positrons are accumulated in cycles of roughly 5 minutes. They are then transferred to the mixing trap with an efficiency of about 50%; here they cool by synchrotron radiation in the 3 T field. The result is a high density ( $1\text{--}2 \times 10^8 \text{ cm}^{-3}$ ) spheroidal positron plasma with a length of about 30 mm and a diameter that can vary from  $\sim 4\text{--}8$  mm. The average positron plasma characteristics measured during the cooling measurements using a plasma mode analysis technique [10,11] were: radius,  $r \sim 2.8$  mm, density,  $n \sim 1.1 \times 10^8 \text{ cm}^{-3}$  and aspect ratio  $\alpha \sim 5.5$ .

The catching trap is a Penning–Malmberg trap in which antiprotons, supplied by the CERN antiproton decelerator (AD) [12], are trapped and then cooled by Coulomb collisions in an electron cloud. Antiprotons, together with the electrons, are subsequently transferred to the adjacent mixing region, and the electrons removed by applying fast, pulsed electric fields. As a result about  $10^4$  antiprotons are available for mixing with the positrons [1].

### 2.1. The nested trap, mixing antiprotons with positrons

The technique used to mix the antiproton and positron clouds is based on the so-called nested po-

\* Corresponding author.

*E-mail address:* alessandro.variola@cern.ch (A. Variola).

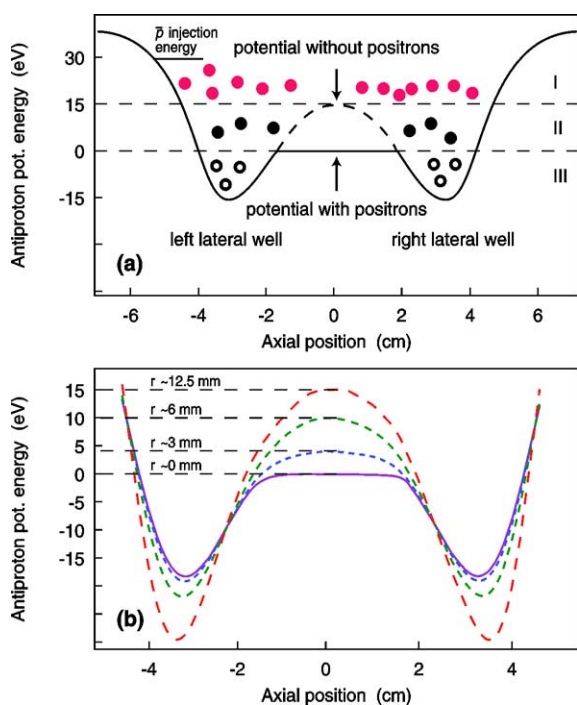


Fig. 1. (a) Potential energy diagrams for antiprotons on the axis of the nested trap are illustrated both with (solid line) and without (dashed line) positrons. The energy regions I to III described in the text are indicated. (b) Potential energy diagrams at different radii.

tential configuration [13], which permits simultaneous axial confinement of oppositely charged particles (Fig. 1(a)). In the ATHENA nested trap, cold positrons are confined in the region that constitutes the central well. Note that the positron space charge effectively flattens the on-axis potential in the mixing region [14]. The space charge potential has been calculated using the positron plasma parameters given by the mode analysis measurements. For the purposes of discussion we will take this flattened level to be the zero of antiproton energy. Antiprotons with negative energies are axially separated from the positron cloud and cannot recombine. It is important to stress that the zero energy level is dependent on the applied and space charge potentials and varies across the radius of the trap. This radial dependence has been calculated and is illustrated in Fig. 1(b) where the nested potential configurations for different radii are shown. In the following we consider mainly the longitudinal motion referring to the on-axis antiprotons; the effects of their

radial distribution and off-axis potential variations will be pointed out when they play a role in the analysis.

To initiate antihydrogen production, a bunch of antiprotons is injected into the mixing trap at  $\sim 30$  eV (arrow in Fig. 1(a)). When the positron plasma is in thermal equilibrium with the environment we call this procedure “cold mixing”. In ATHENA it is also possible to control the positron plasma temperature during the mixing by exciting its axial dipole mode resonance (at around 20 MHz) [11]. A radio-frequency drive with a 2 MHz span across the dipole mode at a sweeping frequency of  $\sim 1$  kHz was applied. The resulting shift in the quadrupole frequency provides the magnitude of the plasma temperature change. When antiprotons are injected into a positron plasma heated to  $\sim 3000$  K, the cycle is termed as “hot mixing”.

### 3. Antiproton cooling measurement technique

After injection the antiprotons traverse the cold positron cloud and lose energy through Coulomb collisions. To measure the energy spectrum of the antiprotons the confining potential is reduced in steps and the annihilation of the released antiprotons is recorded at each step. Fig. 2 shows the sequences employed; the delay between the different potential configurations is  $\sim 100$   $\mu$ s and the duration of every step is  $\sim 50$   $\mu$ s. The energy resolution is determined by the step size of the confining potential and is of the order of a few eV, depending on the detailed potential configuration of each step. The charged pions produced by antiproton annihilation are counted by means of a scintillator system read by photomultipliers. The read out system has a dual pulse resolution of  $\sim 50$  ns. The signals are then recorded with a multi-scaler module which links the delay of the dump with the antiproton energy in the nested trap.

The antiproton dump takes place in two different stages, namely a left well dump (LWD, see Fig. 2(a)) and a subsequent right well dump (RWD, see Fig. 2(b)). In the LWD, all antiprotons with positive energies as well as those in the left well with negative energies are released sequentially. In the RWD, only those antiprotons in the right well with negative energies are released. The positrons are also released during the RWD. The above-mentioned procedure al-

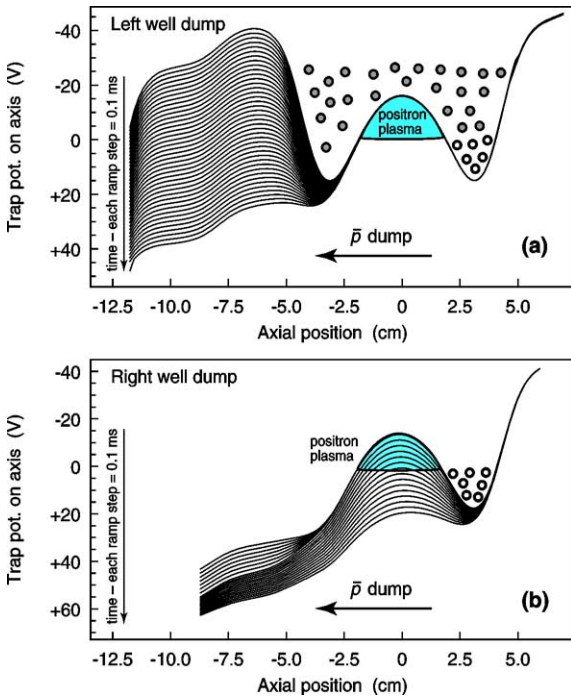


Fig. 2. Schematic of the different on-axis potentials making up the two ramps used for the dump. The antiprotons dumped during the first ramp are indicated in grey, the ones dumped during the second one are represented in white. For clarity, only every other step of the ramp is shown.

allows a single snapshot of the antiproton energy spectrum to be obtained. To derive the time evolution of the antiproton energy distribution during the cooling process we performed series of measurements where the particles were dumped in a controlled manner at various pre-determined times after injection. During these measurements the reproducibility of the positron plasma characteristics was assured by the mode analysis diagnostics.

4. Results

Fig. 3 shows the results of measurements in which the antiproton energy was measured as a function of the interaction time during cold mixing. By integrating the appropriate equation of motion we have taken into account the correction to the antiproton energy due to the time-varying potentials during the ramp. This

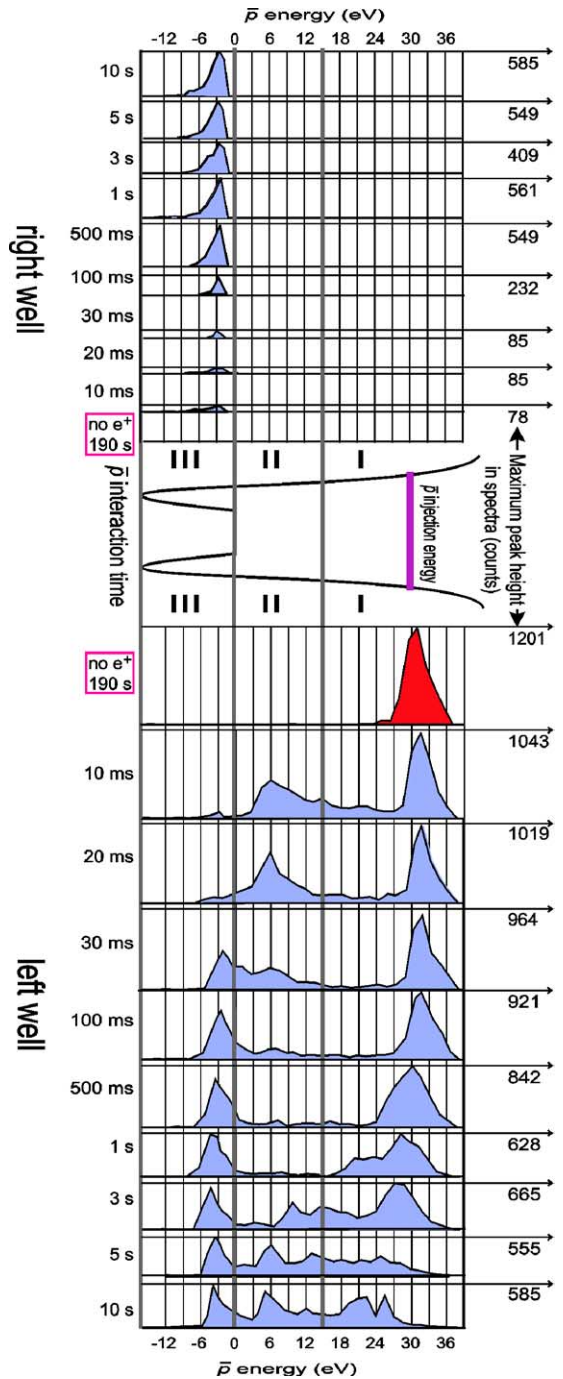


Fig. 3. Antiproton energy spectra for different interaction times. The interaction time is shown on the left, the maximum peak height in each distribution is indicated on the right. The vertical thick grey lines divide the three energy regions. The measurements shown here are cross-normalized using the measured AD beam intensity [8].

effect is often referred to as “adiabatic cooling” and here leads to a correction of no more than 10%.

As a control, a measurement was performed without positrons in the central well (labelled as “no  $e^+$ ” in Fig. 3); the antiprotons were dumped after  $\sim 180$  s, which is the standard antiproton–positron mixing time during antihydrogen production runs. Note that all of the antiprotons are released during the LWD, they remain at the injection energy and the RWD is empty: no cooling is observed. This confirms that our procedure for removal of the cooling electrons, outlined above, is effective. We observe that antiproton cooling to the bottom of the lateral wells only occurs in the presence of electrons, and should not be mistaken for positron cooling.

The remaining spectra in Fig. 3 show the energy distributions for different interaction times. Those below the curve representing the nested well axial potential show the results of the LWD; those above it the RWD.

In general, a redistribution of antiprotons from the injection energy to lower energies is a clear indication that cooling takes place. Qualitatively, the data separate into three distinct energy ranges: I, the injection and cooling region at about 15–40 eV, II, an intermediate region between 0 and  $\sim 15$  eV, and III, the negative energy region of the two lateral wells. The border between region I and II is chosen in a way that radial effects due to off-axis potential variations can be taken into account; under experimental conditions this assures that all the antiprotons that are in thermal equilibrium with the positron plasma but not on the trap axis are included in region II (see Fig. 1(b)).

In our simplified picture the dynamics can thus be discussed in terms of the redistribution of particles between these regions. To do this quantitatively, we determine the fraction of antiprotons remaining in each energy region as a function of interaction time for the “cold” and the “hot” mixing cycles (Fig. 4(a) and (c) respectively: note the logarithmic time scale). We stress that this is only a cooling process diagnostic. Since the normalization is done with respect to the total number of remaining antiprotons all the information on the antiprotons not present in the dump, due to losses or antihydrogen production, are lost in this analysis. The correlation between the different cooling phases and antihydrogen production is established by examining the background-corrected trigger rate

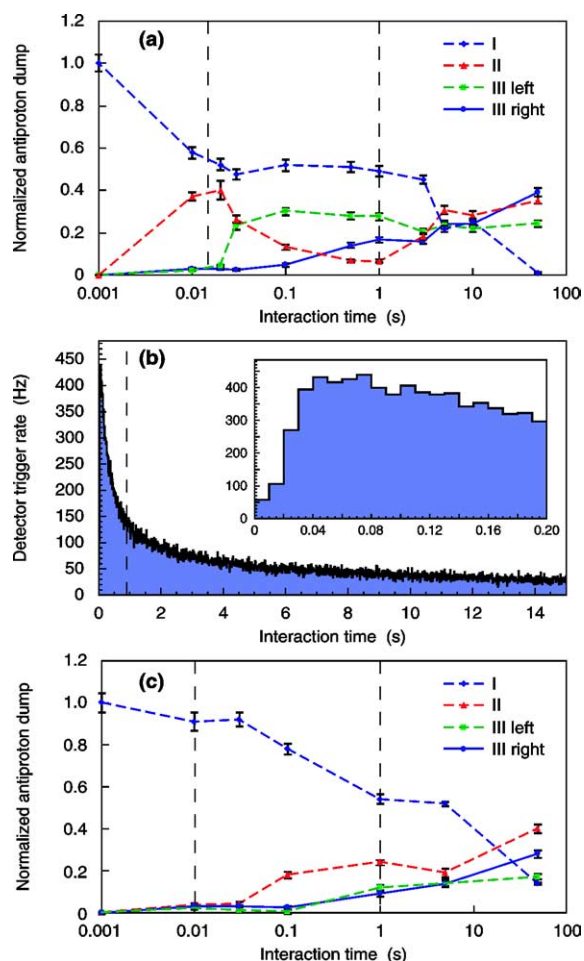


Fig. 4. (a) Fraction of remaining antiprotons in each energy range as a function of the interaction time for cold mixing. (b) Detector trigger rate for a standard cold mixing cycle (background corrected) as a function of time. The inset shows an expansion of time between 0 and 0.2 seconds illustrating the onset of antihydrogen production at  $\sim 20$  ms. (c) Same analysis as in (a) for a  $\sim 3000$  K positron plasma. The lines are to guide the eye. The vertical dotted lines indicate the three time intervals discussed in the text.

of the annihilation detector against interaction time (Fig. 4(b)). Our analysis has shown the trigger rate to be a good proxy for antihydrogen production and subsequent annihilation [15]. Furthermore, it was shown that on average around 65% of the cold mixing cycle trigger rate is due to antihydrogen formation with a peak of the production in the first second where, in a trigger rate signal greater than 300 Hz,  $\sim 85\%$  is identified as antihydrogen. We estimate that about 15% of

the injected antiprotons are converted into antihydrogen atoms that can escape the potentials and be detected by the detector [15]. The background is constituted by antiprotons annihilating on residual gas molecules, with an average trigger rate of a few Hz.

Both sets of data indicate three distinct time scales of evolution. In the first stage, for  $t \lesssim 20$  ms, Fig. 4(a) shows that about 40% of the injected antiprotons are rapidly cooled to region II with an initial cooling rate of about  $2.5 \text{ keV s}^{-1}$ . The inset of Fig. 4(b) illustrates that there is a much reduced antihydrogen production during this fast cooling phase. For intermediate times ( $20 \text{ ms} \lesssim t \lesssim 1 \text{ s}$ ), the evolution is characterized by a loss of population in region II and a growth in the number of antiprotons in the lateral wells (region III), in which the antiprotons no longer have spatial overlap with the positrons. The transition zone between regions II and III is the energy range in which the antiprotons are near to thermal equilibrium with the positrons and therefore have a high probability of recombination (see Section 4.2). The inset in Fig. 4(b) shows the onset and sharp rise in antihydrogen production between 20 and 30 ms. Finally, for  $t \gtrsim 1 \text{ s}$ , we note a slow feeding of antiprotons from region I into the other energy regions, resulting in all antiprotons ending up in regions II or III by about  $t = 50 \text{ s}$ . As Fig. 3 indicates, this time range is characterized by energy loss and spreading of the remaining “hot” injected antiprotons. The time constant is very long compared to those of the previous stages. In this time range Fig. 4(b) shows a decrease of the trigger rate.

We can gain some general insights from the above observations for each stage, as follows.

#### 4.1. Phase 1—fast cooling

The fast cooling time constant ( $t \sim 10 \text{ ms}$ ) for around 40% of the antiprotons is consistent with the  $\sim 4 \text{ ms}$  timescale that is expected for  $\sim 40 \text{ eV}$  antiprotons to thermalize [16,17], when taking into account the time spent outside the positron plasma.<sup>1</sup> The cooling time is strongly dependent on the antiproton relative velocity [16,17] which explains its reduction be-

tween 10 and 20 ms (see Figs. 3, 4). Once thermal equilibrium is approached the antiprotons are able to diffuse inside the positron cloud. Consequently, the time spent in the plasma increases, enhancing the antihydrogen formation probability. Indeed, it is at the end of the fast cooling period that the observed antihydrogen production starts to rise rapidly and peaks after some tens of ms (Fig. 4(b)). The most likely explanation for the fact that only  $\sim 40\%$  of the antiprotons participate in this initial cooling is the incomplete radial overlap between the positron plasma and the antiproton cloud.

Note that in the ATHENA experimental conditions, in the fast cooling process, the deposition of the entire kinetic energy of the injected antiprotons into the positron cloud would only raise the positron temperature by about 25 K without affecting their dynamics. This was confirmed by monitoring the plasma with the modes analysis technique [11]. In the intermediate time range, we expect that the energy deposited in the positron plasma is removed by synchrotron radiation within  $\sim 0.5 \text{ s}$ .

#### 4.2. Phase 2—thermal equilibrium

In Fig. 3 we observe that between 20 and 30 ms, the distribution of cooled antiprotons shifts to lower energies very close to zero and even begins to cross the on-axis potential characteristic of thermal equilibrium between the positrons and antiprotons. As stated earlier, this is the time at which we observe a very rapid increase in antihydrogen production (Fig. 4(b)). Fig. 4 shows that there is a corresponding decrease in the region II population in favor of region III where the two antiparticles are axially separated. While the cross-over from region II to region III depends on the exact position of this border in the left-well dump, with its inherent calibration uncertainty ( $\sim 2 \text{ V}$  determined by the dump step size), it is clear also from the right-well dump that at around this time some antiprotons attain negative energies and are thus separated from the positrons. We suggest two possible contributing factors for this:

- (1) stochastic feeding of antiprotons into the lateral wells due to collisions in the lateral wells that transfer energy from the longitudinal to the radial motion;

<sup>1</sup> Following their dynamics during the fast cooling by means of a numerical code, we found that the antiprotons spend  $\sim 1/3$  of the total time inside the positron plasma.

- (2) production of axially moving weakly bound Rydberg antihydrogen atoms [2], which can be ionized at the longitudinal extremes of the nested potential, trapping the antiproton in the lateral wells.

If we roughly estimate the ATHENA experimental conditions for the antiprotons, i.e., density  $n \sim 10^4 \text{ cm}^{-3}$ , average speed  $\sim$  of a few  $10^3 \text{ ms}^{-1}$  (taking into account the dynamics in the lateral wells), the maximum antiproton–antiproton collision rate  $nvb^2$  (where  $b$  is the classical distance of minimum approach) is of the order of a few Hz. This cannot explain the rapid rise of the lateral well population in the first 500 ms. Thus, one possibility is that the lateral well antiprotons arise mainly due to ionized weakly bound Rydberg antihydrogen atoms. Moreover, the observation that these antiprotons end up with energies in a narrow band just below zero, thereby coinciding with the maximum electric fields for stripping the weakly bound antihydrogen atoms, would seem to corroborate the importance of this mechanism for producing axially separated antiprotons.

That some axial separation takes place has been confirmed by a dedicated re-injection experiment. The length of the lateral wells was adiabatically compressed (by varying the applied potentials) after they were filled. This led to an adiabatic heating [18] of a fraction of the separated antiprotons resulting in their re-injection into the positron plasma where they can recombine.

The result is shown in Fig. 5, where the trigger peak corresponding to the formation of antihydrogen on re-injection is evident. Detailed analysis using the ATHENA vertex detector confirms the production of antihydrogen upon re-injection.

#### 4.3. Phase 3—slow cooling

For  $t \gtrsim 1 \text{ s}$ , it is evident that there is cooling of the antiprotons that still populate region I (radially separated) with a very long time constant. This slow cooling phase could be due to essentially two causes.

- (1) The first is cooling in the tails of the radial distribution of the positron plasma, where the rate is much lower than in the plasma center. According to cold fluid theory [19], the radial tails have an extent equal to the Debye length which, at

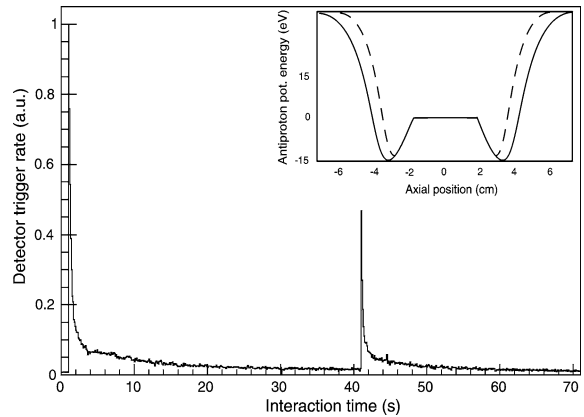


Fig. 5. Trigger rate during re-injection after 40 s. The corresponding peak is mainly due to antihydrogen production. In the inset, the on-axis potentials applied to re-inject the antiprotons into the positron plasma, are displayed (dashed lines).

the ATHENA positron plasma density and temperature conditions, is a few tenths of microns. This cannot explain the large effect evident in the experimental data. However, it is possible that cold fluid theory might not be strictly valid for the ATHENA case of a two component plasma. If we consider centrifugal separation [20] of the positrons and antiprotons, the ATHENA parameters correspond to the partial separation regime. This would significantly alter the tails of the positron distribution. It should be noted though, that centrifugal separation usually only deals with same sign charged plasmas. Understanding of the detailed dynamics of centrifugal separation for oppositely charged plasmas in a nested trap probably await additional theoretical work. The effect needed to explain the slow cooling observed in our measurements does not need to be very large. A density tail in the distribution of  $10^{-3}$  to  $10^{-4}$  over a length scale of the order of the plasma radius outside the positron plasma would be sufficient.

- (2) Supposing that the antiprotons radius is conserved in the nested trap, another source of the slow cooling could be a slow radial expansion of the positron plasma that gradually envelops the initially radially separated antiprotons. This radial transport has been investigated in ATHENA. In our normal experimental conditions (i.e., those pertaining to the data shown in Figs. 3 and 4),

monitoring the positron plasma radius with the mode analysis technique [11], we observe an expansion of roughly 0.1 mm in the first 10 s and of  $\sim 0.25$  mm in the full cycle of 180 s. It should be noted that this expansion does not significantly affect the space charge potential of the positron plasma.

Two other experimental observations indicate that the slow cooling takes place on the initial radially separated antiprotons:

- (a) Strong evidence is given by measurements performed when the positron plasma shape was altered by applying a rotating wall electric field [21] and the antiprotons were dumped 10 ms after injection. The rotating wall was used both in expansion and compression mode. The results are shown in Fig. 6. The peak in region II represents the antiprotons that radially overlap the positron cloud (i.e., are cooled) while region I represents the radially separated antiprotons. The peak in region II is enhanced when the positron plasma is expanded while it almost disappears when the plasma is radially compressed. Furthermore, there are more than twice as many antiprotons in region I after compression than after expansion. The redistribution between these two regions reflects the degree of radial overlap between the antiproton cloud and the positron plasma.
- (b) In Fig. 3, for long interaction times, a second peak is formed in region II. The energy separation between the zero energy level and the peak is  $\sim 5$ – $6$  eV. This is compatible (within the experimental accuracy of  $\sim 2$  V) with the 4 V that separates the potential on axis with the one at a radius of  $\sim 3$  mm (see Fig. 1(b)).

Fig. 4(a) shows that the percentage of region I antiprotons decreases slowly to zero, mostly in favor of the region II, providing a slow source of new antiprotons for antihydrogen production. Looking at the detector trigger rate, for  $t > 1$  s, we observe antihydrogen production decaying with a time constant of about 50 s indicating a possible slow feeding of antiprotons to the positron plasma. It is also important to note that in Fig. 3, the position of the region III peak right well population remains stable during the whole process.

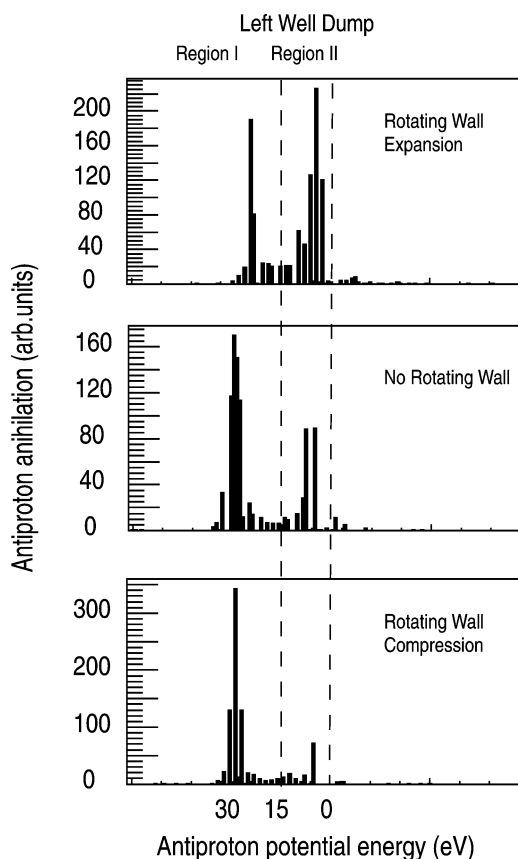


Fig. 6. Antiproton dump results for three different positron plasma characteristics: expanded ( $\alpha \sim 7$ ), not compressed ( $\alpha \sim 20$ ), compressed ( $\alpha \sim 80$ ). The differences in the peak in region II are evident. In the first case 40% of the population is in region I and 60% in region II. A substantial difference is noticed when the rotating wall was not applied: 71% of the antiprotons are in region I and only 29% in region II. This behavior is enhanced by compressing the plasma: 83% of the antiprotons are in region I and 17% in region II.

This supports the contention that other mechanisms of cooling (e.g., due to electrons) are absent during the mixing procedure.

#### 4.4. Heated positron plasma

We have compared the above results to those obtained by repeating the experiment with a heated ( $T \sim 3000$  K) positron plasma (“hot mixing”). Fig. 4(c) illustrates the results of this measurement. The initial cooling is about a factor of 100 slower, the region I antiprotons declining to  $\sim 60\%$  of the initial value in about  $\sim 1$  s. This observation is also in good agreement

with theory [16] where the estimated cooling time is  $\sim 0.4$  s. There is no subsequent loss of region II antiprotons, suggesting that the positron plasma heating effectively inhibits the recombination process. Indeed, we observe that antihydrogen production is strongly suppressed under these conditions [3]. After 50 s about 20% of the hot antiprotons have still not cooled.

## 5. Summary and discussion

In summary, we have studied positron cooling of antiprotons in a previously unexplored regime of positron number and density. Although many observations still have to be better understood, some general features of the cooling process have been identified, their link with antihydrogen production assessed and explanations for the antiproton behavior suggested. For mixing with cold positrons, we observe rapid cooling ( $t \sim 10$  ms) to energies corresponding to thermal equilibrium of the two populations. After this we notice a rapid onset of antihydrogen production with rates exceeding 300 Hz during the first second. On a longer timescale ( $t > 1$  s) a slower cooling process is observed, consistent with the decay of antihydrogen production characterized by a 50 s time constant.

The following conclusions can be drawn from these observations:

- Antihydrogen production starts after the antiproton population has been cooled close to thermal equilibrium.
- Initially only the antiprotons that radially overlap with the positron cloud are cooled and quickly recombine.
- After about 500 ms a small fraction of the antiprotons start to axially separate. These then contribute to the lateral wells population. Re-injection and additional recombination of antiprotons can be obtained by squeezing the length of the lateral wells (adiabatic heating).
- Those antiprotons which are initially radially separated from the positrons cool slowly possibly due to tails in the positron distribution or the slow radial expansion of the positron plasma. This provides a new source of antiprotons suitable for antihydrogen formation.

- When the positron plasma is heated to  $\sim 3000$  K the initial cooling is about a factor of 100 slower, and no antihydrogen production is observed.

Thus, the analysis provides a consistent picture of charged particle dynamics and production of antihydrogen, including the effect of heating the positrons. Further understanding of the positron–antiproton interaction may be obtainable by numerical simulation of the interaction dynamics, but crucial information about the antiproton radial density distribution is currently lacking. A complete understanding of the processes involved would be valuable in optimizing the antihydrogen production rate and the antihydrogen energy distribution. In this goal a next step may be the study of antihydrogen production as a function of the energy of injection of the antiprotons. Also of interest for future experiments is the dependence of the cooling dynamics on the antiproton–positron ratio. It is therefore important to consider the energetics of positron cooling of a much larger number of antiprotons, in order to optimize their reaction rate.

## Acknowledgements

This work was supported by the INFN (Italy), CNPq (Brazil), MEXT (Japan), RIKEN (Japan), SNF (Switzerland), SNF (Denmark) and the EPSRC (UK).

## References

- [1] M. Amoretti, et al., *Nature (London)* 419 (2002) 456.
- [2] G. Gabrielse, et al., *Phys. Rev. Lett.* 89 (2002) 213401.
- [3] M. Amoretti, et al., *Phys. Lett. B* 583 (2004) 59.
- [4] G. Gabrielse, et al., *Phys. Lett. B* 507 (2001) 1.
- [5] H. Higaki, et al., *Phys. Rev. E* 65 (2002) 046410.
- [6] C. Regenfus, *Nucl. Instrum. Methods A* 501 (2003) 65.
- [7] M. Amoretti, et al., *Nucl. Instrum. Methods A* 518 (2004) 679.
- [8] M.C. Fujiwara, M. Marchesotti, *Nucl. Instrum. Methods A* 484 (2002) 162.
- [9] L.V. Jørgensen, et al., in: F. Anderegg, L. Schweikhard, C.F. Driscoll (Eds.), *Nonneutral Plasma Physics IV*, AIP Conf. Proc. 606 (2002) 35.
- [10] M. Amoretti, et al., *Phys. Rev. Lett.* 91 (2003) 055001.
- [11] M. Amoretti, et al., *Phys. Plasmas* 10 (2003) 3056.
- [12] S. Maury, *Hyperfine Interact.* 109 (1997) 43.
- [13] G. Gabrielse, et al., *Phys. Lett. A* 129 (1988) 38.
- [14] J.J. Bollinger, D.J. Wineland, D.H.E. Dubin, *Phys. Plasmas* 1 (1994) 5.

- [15] M. Amoretti, et al., *Phys. Lett. B* 578 (2004) 23.
- [16] L. Spitzer, *Physics of Fully Ionised Gases*, Interscience, New York, 1962.
- [17] Y. Chang, C.A. Ordonez, *Phys. Rev. E* 62 (2000) 6.
- [18] B.R. Beck, Ph.D. Thesis, University of California, San Diego, CA, 1990.
- [19] L. Turner, *Phys. Fluids* 30 (1987) 3196.
- [20] T. O'Neil, *Phys. Fluids* 24 (1981) 1447.
- [21] X.-P. Huang, et al., *Phys. Rev. Lett.* 78 (1997) 875.